9

Antenna Array Design in Aperture Synthesis Radiometers

Jian Dong and Qingxia Li
Huazhong University of Science and Technology
Wuhan, China
dongjian@smail.hust.edu.cn, qingxia_li@mail.hust.edu.cn

1. Introduction

During the past few decades, there has been growing interest in the use of microwave and millimeter wave radiometers for remote sensing of the Earth. Due to the need of large antennas and scanning mechanism, the conventional real aperture radiometer becomes infeasible for high spatial resolution application. Interferometric aperture synthesis was suggested as an alternative to real aperture radiometry for earth observation [Ruf et al., 1988]. Aperture synthesis radiometers (ASR) can synthesize a large aperture by sparsely arranging a number of small aperture antennas to achieve high spatial resolution without requiring very large and massive mechanical scanning antenna.

The fundamental theory behind aperture synthesis technique is the same as the one used for decades in radio astronomy [Thompson et al., 2001], in which the product of pairs of small antennas and signal processing is used in place of a single large aperture. In aperture synthesis, the coherent product (correlation) of the signal from pairs of antennas is measured at different antenna-pair spacings (also called baselines). The product at each baseline yields a sample point in the Fourier transform of the brightness temperature map of the scene, and the scene itself is reconstructed by inverting the sampled transform.

This chapter addresses the subject of antenna array design in ASR, which plays an important role in radiometric imaging of ASR. The chapter is organized as follows. In section 2, the basic principle of synthetic aperture radiometers is briefly formulated. In section 3, the topology optimization of the antenna array is concerned, aiming at minimum redundancy arrays (MRAs) for high spatial resolution. For one-dimensional case, different optimization methods for finding out minimum redundancy linear arrays (MRLAs) such as numerical algorithms and combinatorial methods are summarized, including their advantages and disadvantages. We also propose an effective restricted search method by exploiting the general structure of MRLAs. For two-dimensional case, different antenna array configurations as well as their spatial sampling patterns are compared, including rectangular sampling arrays, hexagonal sampling arrays, and nonuniform sampling arrays. Some original work on the design of thinned circular arrays is also described.

In section 4, a novel antenna array for our HUST-ASR prototype is presented, which is a sparse antenna array with an offset parabolic cylinder reflector at millimeter wave band.

The overall specifications, architecture design, performance evaluation, and measurement results of the antenna array are all detailed. Section 5 presents some experiment results with HUST-ASR, which indicate good capability of imaging natural scenes with high spatial resolution provided by the antenna array. Finally, section 6 concludes this chapter and suggests the further research.

2. Principle of Aperture Synthesis Radiometers

The aperture synthesis radiometer measures the correlation between the signals collected by two spatially separated antennas that have overlapping fields of view, yielding samples of visibility function V, also termed visibilities [Ruf et al., 1988], of the brightness temperature T of the scene under observation. For ideal situation, the relationship between V and T is given by

$$V(u,v) = \iint_{\xi^2+\eta^2\le 1} T(\xi,\eta) e^{-j2\pi(u\xi+v\eta)} d\xi d\eta \tag{1}$$

where (u,v) is the baseline and is equal to the difference between the antenna positions over the XY plane normalized to the wavelength; $T(\xi,\eta)$ is the so-called modified brightness temperature [Camps, 1996].

$$T(\xi,\eta) = \frac{T_B(\xi,\eta)}{\sqrt{1-\xi^2-\eta^2}} F_{n1}(\xi,\eta) F_{n2}^*(\xi,\eta) \tag{2}$$

where $T_B(\xi,\eta)$, dimensions of Kelvin, is the actual apparent brightness temperature; (ξ,η) are the direction cosines, with respect to the (X,Y) axes, equal to $(\sin\theta\cos\varphi, \sin\theta\sin\varphi)$; $F_{n1,2}(\xi,\eta)$ are the normalized antenna voltage patterns.

In the ideal case of identical antenna patterns $F_{n1} = F_{n2} = F_n$, the modified brightness temperature can be recovered by means of an inverse Fourier transform of the visibility samples, that is

$$T(\xi,\eta) = F^{-1}[V(u,v)] \tag{3}$$

In practice, antennas can not be placed continuously; therefore, the measured visibilities are actually the discrete samples of visibility function, so

$$T(\xi,\eta) = \sum_i \sum_j V(u_i,v_j) e^{j2\pi(u_i\xi+v_j\eta)} \tag{4}$$

More generally, the relationship between V and T can be expressed as discrete matrix equation [Tanner, 1990]

$$V = GT_B \tag{5}$$

where G is a matrix, V is visibility vector, and T_B is brightness temperature vector.

G matrix is taken as a spatial impulse response of a synthetic aperture radiometer and can be exactly measured. In measurement, a noise source is placed at one end of the antenna range, and the radiometer is rotated in azimuth at the other end of the range in such a way as to scan the point source across the field of view.

When the aperture synthesis radiometer observes a scene, the brightness temperature image can be inverted by the Moore-Penrose pseudo-inverse [Tanner & Swift, 1993]

$$T_B = G^T (GG^T)^{-1} V \tag{6}$$

which is used as the basis in our inversion process.
Different from the simple Fourier transform expressed by (1) and (3), the measured G matrix contains the information of errors in the radiometer system, such as individual antenna patterns, obliquity factors, and fringe-washing functions. When G matrix is used to reconstruct images, part of errors in the system is actually corrected.

3. Topology Design of Antenna Arrays in Aperture Synthesis Radiometers

As a crucial technique for aperture synthesis radiometers (ASR), antenna array design plays an important role in radiometric imaging. Usually, antenna array design in ASR aims to find the minimum redundancy array (MRA) [Ruf et al., 1988; Ruf, 1993; Camps et al., 2001], which can provide the most uniform and complete (u, v) coverage in the Fourier plane with the given number of antenna elements and therefore achieves the highest spatial resolution of the image. In view of different manufacturing difficulties in antenna engineering and different mutual coupling, various candidates of array configurations with similar spatial resolution are also desirable in practical applications. Except for interferometric aperture synthesis radiometry, MRA is also widely used in adaptive beamforming [Jorgenson et al., 1991; Dong et al., 2008b], spatial spectrum estimation [Pillai et al., 1985], and radar imaging [Chen & Vaidyanathan, 2008; Dong et al., 2009c].
On the other hand, the radiometric sensitivity, as one of the most crucial specifications of synthetic aperture radiometers, must also be taken into account in the antenna array design. For remote sensing from space, especially from a moving platform such as low Earth orbit satellite and aircraft, too thinned arrays would much worsen the radiometric sensitivity of ASR, so a tradeoff must be made between thinning of the array (to reduce the size and weight in orbit) and obtaining the required sensitivity [Le Vine, 1990]. The sensitivity of ASR depends much on antenna array configurations because of different (u, v) spatial frequency samples and different levels of redundancy associated with array configurations [Ruf et al., 1988; Camps et al., 1998; Butora & Camps, 2003]. The problem of how to properly arrange antenna elements to achieve the optimum sensitivity of ASR is an interesting issue, on which no dedicated research has been found up to date. Detailed research on this issue is carried out by the authors and the results are presented in [Dong et al., 2009e], where the minimum degradation array (MDA) is suggested for the optimum radiometric sensitivity of ASR, and methods are proposed to search for MDA.
In this section, we only address the subject of MRA design for high spatial resolution, in which different optimization methods and different array configurations are described.

3.1 Minimum Redundancy Linear Arrays

The problem of finding out optimum MRLA has been first investigated as a purely number theoretic issue of "difference basis" [Redéi & Rényi, 1948; Leech, 1956; Wichman, 1963; Miller, 1971], in which each antenna of the array is assigned an integer representing its position, the problem then reduces to constructing a set of n integers, called a difference basis, which generate contiguous differences from 1 up to the largest possible number. Leech [1956] presented some optimum solutions for n≤11 and demonstrated that for

optimum MRLA, $1.217 \le R \le 1.332$ for $n \to \infty$, where the redundancy R is quantitatively defined as the number of possible pairs of antennas divided by the maximum spacing L:

$$R = \frac{C_n^2}{L} = \frac{n(n-1)}{2L} \tag{7}$$

where $C_p^q = p!/q!(p-q)!$ is the number of combinations of p items taken q at a time.

It is difficult to find the optimum MRLAs when large numbers of elements are involved because of the exponentially explosive search space, and several earlier attempts as well as our work are detailed as follows.

(a) Numerical search algorithms

For a small number of elements, it is possible to find MRLAs by a simple exhaustive search in solution space; but for a large number of elements, it is computationally prohibitive to do so. With the help of powerful modern computers, some numerical optimization algorithms were proposed to search for MRLAs.

Ishiguro [1980] proposed iterative search methods to construct MRLAs: to start with the configuration of {. 1 . (L-1).} (the integers in the set denote the spacing) and to examine larger spacings preferentially. A site is selected as optimum which, if occupied, gives as many missing spacings as possible. When more than one site is selected as optimum at some stage, they are registered without exception to examine all the combinations of tree structure derived from them. This process is repeated until the condition of full spacing is obtained.

Lee & Pillai [1988] proposed a "greedy" constructive algorithm for optimal placement of MRLA: like Ishiguro's algorithm, in each stage, a site is selected as optimum which, if occupied, gives as many missing spacings as possible. And the results of this stage are stored in a linked list (output linked list), which in turn becomes an input linked list for the next stage. The algorithm needs large computation time and excessive memory storage. To cope with these problems, a modified suboptimal version of this algorithm is also proposed by Lee. With the highly reduced computation time and memory storage, the resulting solution is far from optimality.

As an effective stochastic optimizer, simulated annealing (SA) algorithm was first applied to the search of MRLA by Ruf [1993] and displayed the superiority over Ishiguro's algorithm and Lee's algorithm. The most distinguished property of SA from those local search algorithms is that the algorithm can escape from local minimum wells and approach a global minimum by accepting a worse configuration with a probability dependent on annealing temperature.

Blanton & McClellan [1991] considered the problem of finding MRLA as creating a tree structure of templates, and Linebarger [1992] considered the problem as computing the coarray of MRLA from a boolean algebraic point of view. By combining Linebarger's technique with Blanton's, dramatic speedup in searching MRLA may be expected.

It is worth noting that except for simulated annealing, other global optimizers, such as genetic algorithms (GAs) [Goldberg, 1989] and ant colony optimization (ACO) [Dorigo & Stutzle, 2004], may also be used to search MRLA. Although succeeding in escaping from local minima, the global search for MRLAs with large number of antennas still requires high computational cost because of the exponentially explosive search space. Further consideration is that in order to improve the efficiency of the exploration as much as possible, we might experiment with algorithms with a different combination of randomness and gradient descent.

In summary, although various numerical algorithms were proposed, the contradiction between solution quality and computation efficiency limits practical applications of all these algorithms, i.e. reducing computation time would lead to a poor solution, like Ishiguro's algorithm and Lee's algorithm, while obtaining good solution would require large computation time, like Ruf's algorithm.

(b) Combinatorial methods

Different from numerical search algorithms described above, the combinatorial methods usually need very little computational cost and have closed form solutions.

Ishiguro [1980] proposed a method to construct large MRLA by a recursive use of optimum small MRLA. The method are considered in two cases. In case 1, suppose that an MRLA of n antennas (MRLA1 with the maximum spacing N) are arranged in the array configuration of an MRLA of m antennas (MRLA2 with the maximum spacing M). As a result, a new nm-elment MRLA is synthesized with the maximum spacing

$$L = M(2N+1) + N = 2MN + M + N \tag{8}$$

In case 2, suppose that MRLA2 in case 1 is recursively used k times, the total number l_k of antennas and the maximum spacing L_k are, respectively,

$$l_k = m^{k-1} n \quad (k \geq 2) \tag{9}$$

$$L_k = [(2M+1)^{k-1}(2N+1) - 1]/2 \quad (k \geq 2) \tag{10}$$

By using a small difference basis and cyclic difference set (CDS), a combinatorial method to construct larger difference basis, i.e. MRLA, was described in [Redéi & Rényi, 1948; Leech, 1956]. The method was also reformulated by Kopilovich [1995] and used to design linear interferometers with a large number of elements. Redéi & Rényi and Leech showed that, if a sequence $\{b_i\}$ (i=1,…,r) is a basis for the [0, P] segment (we call it the "initial" basis), and if $\{d_j\}$ (j=1,…,k) is a CDS [Baumert, 1971; Hall, 1986]with parameters V, k, and λ=1, then the set

$$\{d_j + b_i \cdot V\} \tag{11}$$

consisting of K=kr integers, is the difference basis for the segment of length

$$L = (P+1)V - (d_k - d_1) - 1 \tag{12}$$

Thus, using a difference basis for a small segment and a CDS, one can construct a difference basis for a much longer segment. For the same number of elements, this method outperms Ishiguro's method, i.e. having lower redundancy. Moreover, with element number increasing, the redundancy R decreases steadily (though not monotonically) and then stabilizes, while that of Ishiguro's arrays grows. In a general sense, Ishiguro's construction can also be generalized into this combinatorial method, i.e. using two difference bases for small segments, one can construct a difference basis for a much longer segment.

The two combinatorial methods described above cannot provide a solution for any given number of antennas, such as for a prime number of antennas. For any given number of antennas, Bracewell [1966] proposed a systematic arrangement method, which is summarized as follows:

For an odd number of antennas (n=2m+1)

$$\{1^{m+1},(m+2),(m+1)^m\} \tag{13}$$

where i^m denotes m repetions of the interelment spacing i, each integer in the set denotes the spacing between adjacent antennas.
For an even number of antennas (n=2m)

$$\{1^{m+1},(m+2),(m+1)^m\} \tag{14}$$

The values of R for (13) and (14) approach 2 for a large value of n.
Another approach to MRLA design is based on the recognition of patterns in the known MRLA arrays that can be generalized into arrays with any number of antennas. The most successful pattern thus far is given by

$$\{1^p,(2p+2)^{p+1},(4p+3)^l,(2p+1)^p,p+1,1^p\} \tag{15}$$

where p and l are positive integers. This pattern was originally discovered by Wichman [1963] in the early 1960's and also found by Pearson et al. [1990] and Linebarger et al. [1993] later. Proofs that this expression yields an array with no missing spacings are found in [Miller, 1971; Pearson et al., 1990]. The pattern can be shown to produce arrays such that $n^2/L \le 3$ (R<1.5), where n and L are defined as in (7). More similiar patterns satisfying $n^2/L \le 3$ can be found in [Dong et al., 2009d]. Some patterns inferior to these patterns were also listed in [Linebarger et al., 1993], which may be of use under certain array geometry constraints.

(c) Restricted search by exploiting general structure of MRLAs
It is prohibitive to search out all the possible configurations because of the exponentially explosive search space. However, if the configurations are restricted by introducing some definite principles in placing antennas, it is not unrealistic to search out all the possibilities involved in them. Fortunately, there are apparent regular patterns in the configurations of optimum MRLAs for a large value of n, i.e. the largest spacing between successive pairs of antennas repeats many times at the central part of the array. Such MRLA patterns were presented by Ishiguro [1980] and Camps et al. [2001]. Based on previous researcher's work, we summarize a common general structure of large MRLAs and propose a restricted optimization search method by exploiting general structure of MRLAs, which can ensure obtaining low-redundancy large linear arrays while greatly reducing the size of the search space, therefore greatly reducing computation time. Details of the method can be seen in [Dong et al., 2009d].

3.2 Minimum Redundancy Planar Arrays

The main advantage of planar arrays over linear arrays in ASR is that planar arrays can provide the instantaneous spatial frequency coverage for snapshot imaging without any mechanical scanning. In two dimensions the choice of a minimum redundancy configuration of antennas is not as simple as for a linear array. By different sampling patterns in (u,v) plane, the planar arrays can be divided into:
(a) Rectangular sampling arrays
Typical configurations with rectangular sampling are Mills cross [Mills & Little, 1953], U-shape, T-shape, L-shape [Camps, 1996] arrays, where U-shape array was adopted in HUT-

2D airborne ASR for imaging of the Earth [Rautiainen et al., 2008]. Both U-shape and T-shape configurations and their spatial frequency coverage are shown in Fig. 1 , assumed that the minimum spacing is half a wavelength. By ignoring the effect of the small extensions on the left and right sides of the square domain, both arrays have the same area of (u,v) coverage. An optimal T-shape (or U-shape) array (also see in Fig. 1) was proposed by Chow [1971], which has a larger area of (u,v) coverage than the regular T array but results in a unequal angular resolution in each dimension.

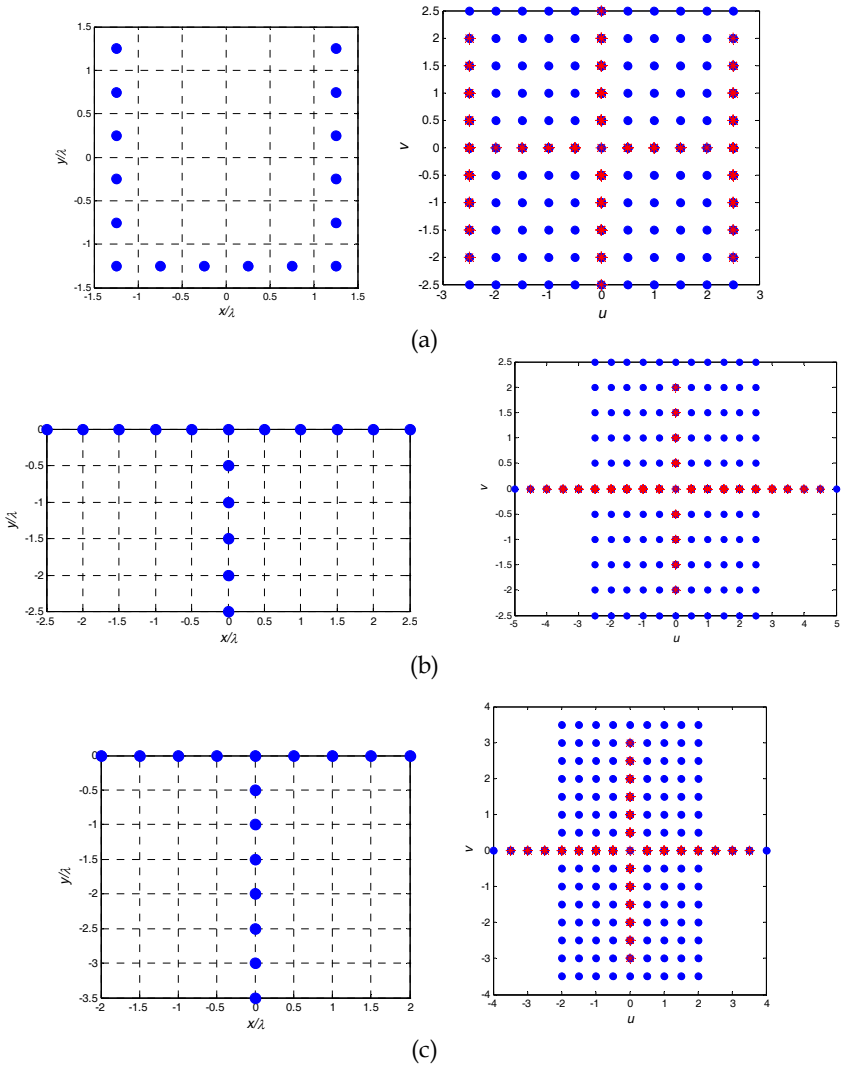

Fig. 1. Different array configurations for rectangular domain and their spatial frequency coverage. Red star points denote redundant (u, v) samples. (a) 16-elment regular U-shape array; (b) 16-elment regular T-shape array; (c) 16-elment optimal T-shape array

A "cross product" planar array can be constructed by "multiplying" two MRLAs: Let $\{a_i\}$ denote the element location set of an MRLA arranged along x axis, and let $\{b_i\}$ denote the location set of an MRLA arranged along y axis, then the location set of the resulting "cross product" planar array is $\{a_i, b_i\}$. An example of a 5×4 "cross product" array is shown in Fig. 2. The authors show [Dong et al., 2009a] that the "cross product" array can obtain more spatial frequency samples and larger (u,v) coverage , therefore achieve higher spatial resolution, compared to U-shape or T-shape array with the same element number.

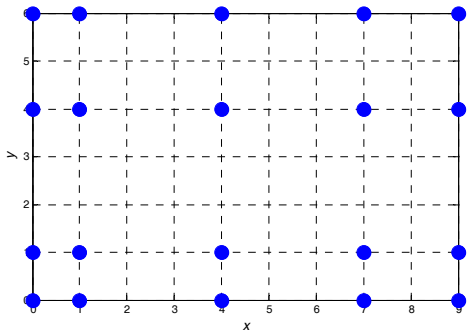

Fig. 2. An example of a 5×4 "cross product" array

A second regular structure, named as Greene-Wood (GW) array, was proposed by Greene & Wood [1978] for square arrays. The element location (i, j) of such an array of aperture L satisfies: i=0 or j=0 or i=j=2,3,…,L. An example of a 12-element GW array with L=4 is shown in Fig. 3.

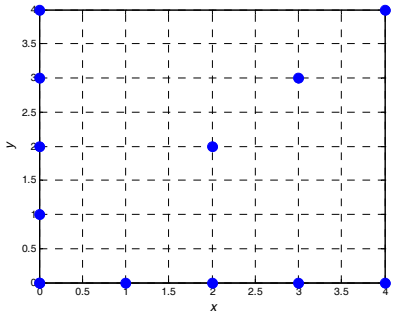

Fig. 3. An example of a 12-element Greene-Wood array with L=4

Two combinatorial methods to construct minimum redundancy arrays for rectangular domain were proposed in [Kopilovich, 1992; Kopilovich & Sodin, 1996]. One method is a generalization of one-dimensional Leech's construction described in section 3.1(b), that is, by multiplying one-dimensional basis of the form in (11), one can obtain the two-dimensional basis consisting of $K = r_1 r_2 k_1 k_2$ elements for the $L_1 \times L_2$ domain,

$$\{d_j + b_i \cdot V_a, d_s^{'} + b_t^{'} \cdot V_b\} \quad \begin{matrix} j = 1, \cdots, k_1; s = 1, \cdots, k_2 \\ i = 1, \cdots, r_1; t = 1, \cdots, r_2 \end{matrix} \tag{16}$$

where $\{d_j\}$ and $\{d_s'\}$ are CDSs with the parameters (V_a, k_1,1) and (V_b, k_2,1) (d_1=d_1'=0 is specified), respectively, while $\{b_i\}$ and $\{b_t'\}$ are the bases for the segment [0, P_1] and [0, P_2]; and $L_1 = (P_1 + 1)V_a - d_{k1} - 1;\ L_2 = (P_2 + 1)V_b - d_{k2}^{'} - 1$.

The other method is based on the concept of two-dimensional difference sets (TDS). Similar to CDS, a TDS with the parameters (v_a, v_b, k, λ) is a set $\{a_i, b_i\}$ of k elements on a (v_a-1)×(v_b-1) grid such that pairs (v_1, v_2) of co-ordinates of any nonzero grid node have exactly λ representations of the form

$$v_1 \equiv a_i - a_j \bmod v_a \quad v_2 \equiv b_i - b_j \bmod v_b \tag{17}$$

If there exists a two-dimensional basis $\{(\gamma_j, \delta_j)\}$ with k_0 elements for a small P_1×P_2 grid and a TDS $\{a_i, b_i\}$ with the parameters (v_a, v_b, k, λ), then the set of K=k×k_0 elements

$$\{(\gamma_j v_a + a_i, \delta_j v_b + b_i)\} \quad i = 1, \cdots k \quad j = 1, \cdots, k_0 \tag{18}$$

forms a basis for the L_1×L_2 grid with

$$L_1 = v_a P_1 + A_0 - 1 \quad L_2 = v_b P_2 + B_0 - 1 \tag{19}$$

where the values A_0 and B_0 depend on the parameters v_a and v_b.

Kopilovich showed that the arrays constructed by both methods outperform T-shape or U-shape array in (u, v) coverage for the same number of elements.

(b) Hexagonal sampling arrays

Hexagonal sampling is the most efficient sampling pattern for a two-dimensional circularly band-limited signal [Mersereau, 1979; Dudgeon & Mersereau, 1984], in the sense that the hexagonal grid requires the minimum density of (u, v) samples to reconstruct the original brightness temperature with a specified aliasing level (13.4% less samples than rectangular sampling pattern). Typical configurations with hexagonal sampling are Y-shape and triangular-shape arrays [Camps, 1996]. Both configurations and their spatial frequency coverage are shown in Fig. 4, assumed that the minimum spacing is $1/\sqrt{3}$ wavelengths. For the similiar number of elements, Y-shape array has larger (u, v) coverage than that for a triangular-shape array, meaning better spatial resolution. On the other hand, triangular-shape arrays cover a complete hexagonal period, while Y-shape arrays have missing (u, v) samples between the star points. Hexagonal fast Fourier transforms (HFFT) algorithms [Ehrhardt, 1993; Camps et al., 1997] are developed for hexagonally sampled data that directly compute output points on a rectangular lattice and avoid the need of interpolations.

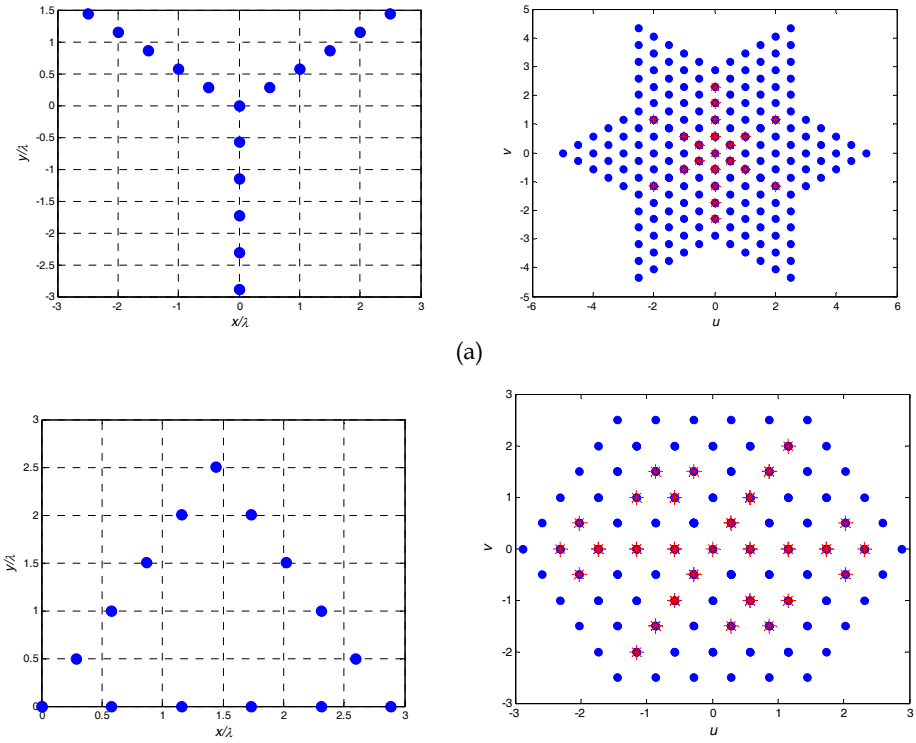

Fig. 4. Different array configurations for hexagonal domain and their spatial frequency coverage. Red star points denote redundant (u, v) samples. (a) 16-element Y-shape array; (b) 15-element triangular-shape array

Y-shape array was adopted in MIRAS [Martín-Neira & Goutoule, 1997] for two-dimensional imaging of the Earth. There are several variations for Y-shape array. Staggered-Y array was proposed for GeoSTAR [Lambrigtsen et al., 2004], which staggers the three arms counter-clockwisely and then brings them together so that the three inner most elements form an equilateral triangle. This Staggered-Y configuration eliminates the need for an odd receiver at the center. The only penalty is a slight and negligible loss of (u, v) coverage. Sub-Y configuration was suggested by Lee et al. [2005] to achieve larger (u, v) coverage at the cost of more incomplete samples than Y-shape array. Its basic unit is a subarray consisting of four elements arranged in Y-shape.

Several sparse hexagonal configurations were suggested in [Kopilovich, 2001; Sodin & Kopilovich, 2001 & 2002]. Like triangular-shape array, they cover a complete hexagonal period. One configuration is to fill up five sides of a regular hexagon of a given radius r by element which provide complete coverage of a hexagonal domain of the double radius in (u, v) plane. A second configuration is that ($3r$+1) elements are arranged equidistantly on three non-adjacent sides of the hexagon while others are arranged inside it. A third configuration, named as three-cornered configurations (TCCs), has three-fold symmetry, i.e. invariant to

rotation by 120°around a certain centre of symmetry. Besides, based on cyclic difference sets (CDSs), Sodin & Kopilovich [2002] developed an effective method to synthesize nonredundant arrays on hexagonal grids.

(c) Non-uniform sampling arrays
Different from those open-ended configurations such as U, T, and Y, there are some closed configurations, such as a circular array and a Reuleaux triangle array [Keto, 1997; Thompson et al., 2001]. A uniform circular array (UCA) produces a sampling pattern that is too tightly packed in radius at large spacings and too tight in azimuth at small. Despite being nonredundant for odd number of elements, the (u, v) samples of a UCA are nonuniform and need to be regularized into the rectangular grids for image reconstruction. One way of obtaining a more uniform distribution within a circular (u, v) area is to randomize the spacings of the antennas around the circle. Keto [1997] discussed various algorithms for optimizing the uniformity of the spatial sensitivity. An earlier investigation of circular arrays by Cornwell [1988] also resulted in good uniformity within a circular (u, v) area. In this case, an optimizing program based on simulated annealing was used, and the spacing of the antennas around the circle shows various degrees of symmetry that result in patterns resembling crystalline structure in the (u, v) samples.
An interesting fact for a UCA is that (u, v) samples are highly redundant in baseline length. Like ULA, a large number of elements can be removed from a UCA while still preserving all baseline lengths. Thus, by several times of rotary measurement, all baseline vectors (both length and orientation) of a UCA can be obtained. Having the advantage of greatly reducing hardware cost, the thinned circular array with a time-shared sampling scheme is particularly suitable in applications where the scene is slowly time-varying. Based on the difference basis and the cyclic difference set in combinatorial theory, methods are proposed by the authors for the design of the thinned circular array. Some initial work on this issue can be found in [Dong et al., 2009b].
The uniform Reuleaux triangle array would provide slightly better uniformity in (u, v) coverage than the UCA because of the less symmetry in the configuration, and optimization algorithms can also be applied to the Reuleaux triangle array to achieve a more uniform (u, v) coverage within a circular area.

4. Antenna Array Design in HUST-ASR

The first instrument to use aperture synthesis concept was the Electronically Scanned Thinned Array Radiometer (ESTAR), an airborne L-band radiometer using real aperture for along-track direction and interferometric aperture synthesis for across-track direction [Le Vine et al., 1994; Le Vine et al., 2001]. An L-band radiometer using aperture synthesis in both directions, the Microwave Imaging Radiometer Using Aperture Synthesis (MIRAS), was proposed by ESA [Martín-Neira & Goutoule, 1997] to provide soil moisture and ocean surface salinity global coverage measurements from space. In 2004, the Geostationary Synthetic Thinned Aperture Radiometer (GeoSTAR) was proposed by NASA [Lambrigtsen et al., 2004] as a solution to GOES (the Geostationary Operational Environmental Satellite system) microwave sounder problem, which synthesizes a large aperture by two-dimensional aperture synthesis to measure the atmospheric parameters at millimeter wave frequencies with high spatial resolution from GEO.

To evaluate the performance of aperture synthesis radiometers at millimeter wave band, a one-dimensional prototype of aperture synthesis radiometer working at millimeter wave band, HUST-ASR [Li et al., 2008a; Li et al., 2008b], is developed at Huazhong University of Science and Technology, Wuhan, China.
The prototype architecture of the millimeter wave aperture synthesis radiometer is shown in Fig. 5. The HUST-ASR prototype mainly consists of antenna array, receiving channel array, ADC array, image reconstruction part. Other parts such as calibration source, calibration and gain control, local oscillator, correlating, error correction are also shown in the figure. As the most highlighted part of HUST-ASR prototype, the antenna array will be detailed in this section, including the overall specifications, architecture design, performance evaluation, and measurement results [Dong et al., 2008a].

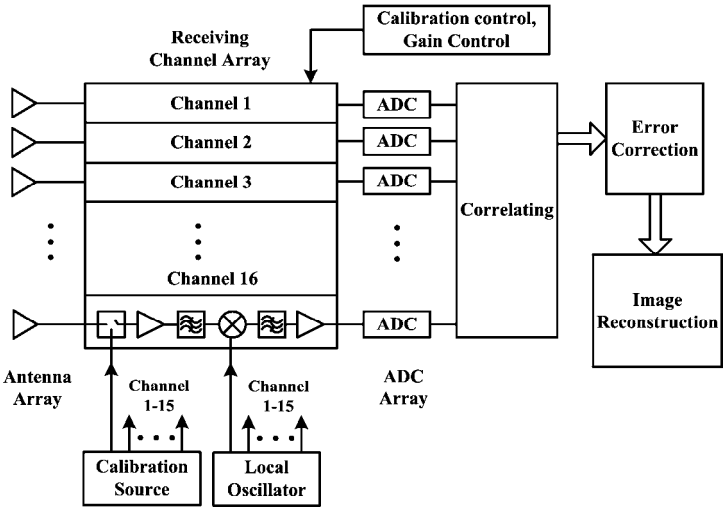

Fig. 5. Prototype architecture of HUST-ASR

4.1 Antenna Array Overall Requirements

One-dimensional synthetic aperture radiometer requires an antenna array to produce a group of fan-beams which overlap and can be interfered with each other to synthesize multiple pencil beams simultaneously [Ruf et al., 1988]. To satisfy this, each antenna element should have a very large aperture in one dimension, while a small aperture in the other dimension.
Due to the high frequency of Ka band, three candidates for the linear array elements were considered among sectoral horns, slotted waveguide arrays and a parabolic cylinder reflector fed by horns. Too narrow bandwidth and mechanical complexity make slotted waveguide arrays less attractive. Sectoral horns with large aperture dimensions would make the length of horns too long to be fabricated. The concept of a parabolic cylinder reflector fed by horns provides an attractive option for one-dimensional synthetic aperture radiometer for several good reasons including wide bandwidth, mechanical simplicity and high

reliability. The massiveness resulting from this configuration may be overcome by lightweight materials and deployable mechanism.
The main design parameters of the antenna array are listed in Table 1.

Frequency Band	8*mm*-band
Bandwidth (GHz)	±2
Sidelobe Level (dB)	<-20
H-plane Beamwidth (deg.)	0.7
E-plane Synthesized Beamwidth (deg.)	0.3
Gain for Each Element (dB)	30
VSWR	≤1.2
Polarization	Horizontal

Table 1. Main design parameters for antenna elements

4.2 Antenna Array Architecture and Design

Fig. 6 simply shows the whole architecture of the antenna array, which is a sparse antenna array with offset parabolic cylinder reflector for HUST-ASR prototype. In essence each HUST-ASR antenna element is composed of a feedhorn and the parabolic cylinder reflector. The elements are arranged in a sparse linear array and thus can share a single reflector.

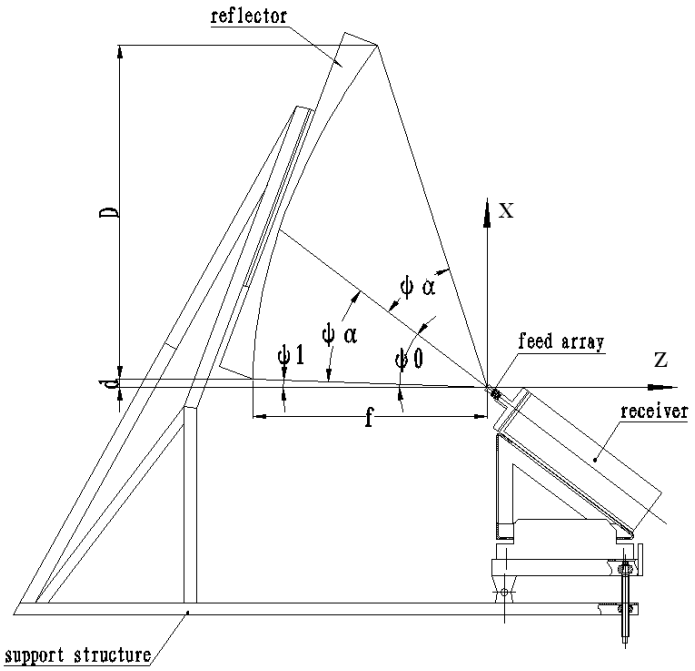

Fig. 6. Artist's concept of the whole antenna architecture

To avoid gain loss due to feed blockage, an offset reflector configuration was adopted. This configuration would also reduce VSWR and improve sidelobe levels [Balanis, 2005; Milligan, 2002]. The ratio of focal length to diameter (f/D) for reflector was determined as 0.7 considering achieving high gain, low cross-polarization level meanwhile maintaining compact mechanical structures. A -12dB edge illumination, not a -10dB edge illumination usually for optimal gain, is designed due to the need for a low sidelobe level. Asymmetric illumination taper on reflector aperture plane due to offset configuration, causing degradation in secondary radiation pattern of the antenna, can be mitigated by adjusting the pointing angle of feed horns.

Different from a conventional uniform linear array, 16 pyramid horns are disposed in a minimum redundancy linear array (MRLA) along the focal line of the reflector to carry out cross-track aperture synthesis for high spatial resolution imaging. The position of each element in the array is shown in Fig. 7. The minimum element spacing between adjacent horns is chosen to be one wavelength ensuring an unambiguous field of view of ±30° from the normal of array axis. The maximum spacing of the feed array is 90 wavelengths. Therefore, the -3dB angular resolution in y direction by aperture synthesis of array elements is

$$\Delta\theta_y = 0.88\frac{\lambda}{D_y} = 0.88\frac{\lambda}{2\cdot 90\lambda} = 0.28^\circ \tag{20}$$

where λ is the wavelength. In (20), The Hermitian of visibility samples [Ruf et al., 1988] is considered to double the maximum aperture of the array (D_y=2×90λ), and therefore double the angular resolution.

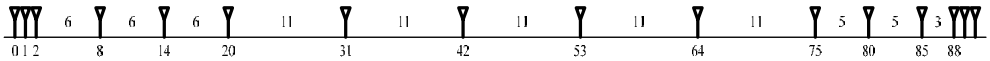

Fig. 7. Arrangement of 16-element minimum redundancy linear array

A delicate support structure connecting the parabolic cylinder reflector and the primary feed array is manufactured as shown in Fig. 6. One side of the support structure serves as back support of the reflector, while the other provides a bevel on which the primary feed array is connected to millimeter wave front-ends of receivers through straight or bent BJ-320 (WR-28) waveguides. By using three pairs of tunable bolts under the bevel, the feed array can be exactly adjusted to the focal line of the reflector.

The specific design features of each part of the whole antenna system are detailed below.

(a) *Reflector Geometry*

To achieve aperture synthesis in one plane, the shape of the reflector is a singly-curved offset parabolic cylinder. This type of reflector has a focal line rather than a focal point. Fig. 6 shows a vertical cross section of the parabolic cylindrical reflector.

The geometric parameters of the parabolic cylindrical reflector are designed referring to [Lin & Nie, 2002; Milligan, 2002] and listed in Table 2. The value of D_x is selected by empirical formula

$$\Delta\theta_x = 1.18\frac{\lambda}{D_x} = 68^\circ\frac{\lambda}{D_x} \tag{21}$$

where $\Delta\theta_x$ is the -3dB angular resolution in x direction, Noticeably, the reflector length L along y direction is large enough to guarantee an E-plane edge illumination level lower than -7dB even for the element at each end of the array.

Aperture Vertical Length D_x	$0.8m$
Aperture Horizontal Length L	$1.8m$
Focal length f	$0.56m$
offset distance d	$0.02m$
Angle, lower rim ψ_1	2.05°
Angle, upper rim ψ_2	72.45°
Bisecting angle ψ_0	37.25°
Subtended half angle ψ_a	35.2°
Edge illumination (EI)	-12dB
Path loss, lower rim PL_1	0.932dB
Path loss, upper rim PL_2	-2.797dB
Path loss, average PL_{ave}	-0.933dB

Table 2. Reflector geometric parameters

(b) *Feed Horn*

The E-plane aperture b of each feed horn is flared as large as possible to about one wavelength in order to reduce VSWR and maximize receiving gain of each element of the antenna array, so a peculiar structure which connects three horns as a whole at each end of the array is used. The H-plane aperture size w of each feed horn is decided according to the specified edge illumination (EI=-12dB) and illumination angle ($2\psi_a$=70.4°) of the parabolic cylindrical reflector. Based on the simulation results shown in Fig. 8 given by HFSS, we choose w=14.8mm, R=25mm, where R is the distance between the aperture plane center and the neck of a horn.

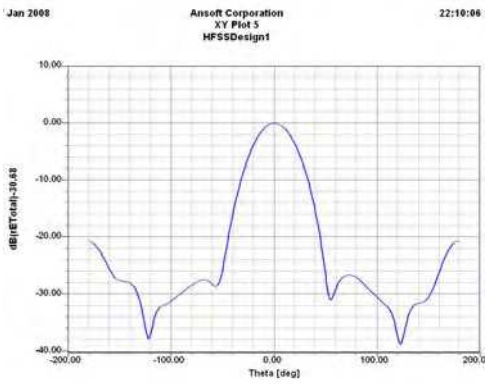

Fig. 8. H-plane radiation pattern simulated by HFSS

(c) *Antenna Tolerance Restrictions*
Antenna tolerance, having great influence on reflector antenna performance, is also considered in our design. The lateral and axial feed array element position errors are restricted to less than 0.2*mm* and 0.12*mm* separately. The RMS value of random surface error is restricted to 0.2*mm*, i.e. less than $\lambda/40$.

4.3 Electrical Performance Evaluation

To validate our design, the fundamental parameters of antenna such as Half-Power Beam Width (HPBW), sidelobe level and gain are evaluated below.

(a) *HPBW and Sidelobe Level*
The Aperture Integral Method [Balanis, 2005] is used to solve far field radiation pattern of our antenna array elements. The projected aperture field distribution of the reflector in the x direction can usually be approximated by the following expression [Lin & Nie, 2002; Milligan, 2002]

$$Q(x) = C + (1-C)[1-(\frac{x-h}{a})^2]^p \tag{22}$$

For our application, $C = 10^{EI/20} = 0.25$, p=1.5, a=$D/2$=0.4m, h=a+d=0.42m.
Assume that the aperture distribution has no variation in the y direction because of a flat profile in that dimension. According to scalar diffraction theory [Balanis, 2005], the far field pattern of the antenna is proportional to the Fourier transform of its aperture distribution and may be expressed as

$$E(\theta,\varphi) = \int_{aperture} Q(\vec{r}) e^{j\vec{k}\bullet\vec{r}} ds \tag{23}$$

Assuming aperture field distribution is separable, from (23) we can approximately calculate the secondary pattern of the antenna in two principal planes.
In H-plane (φ=0°),

$$E(\theta) = \int_d^{d+D} Q(x) e^{jkx\sin\theta} dx \tag{24}$$

In E-plane (φ=90°),

$$E(\theta) = \int_{-b/2}^{b/2} e^{jky\sin\theta} dy \tag{25}$$

From (24) and (25), we can see that the HPBW of H and E plane are about 0.7° and 51°, respectively, and the first sidelobe level of H and E plane are about -23dB and -13.2dB, separately. The sidelobe level of E-plane can be further reduced by array factor of ASR [Ruf et al., 1988].
(b) *Gain*
Using (22), we can get the aperture efficiency

$$\eta_a = \frac{\left[\int_d^{d+D} Q(x)dx\right]^2}{\int_d^{d+D} Q^2(x)dx} \approx 0.88 \tag{26}$$

Due to a flat profile in the y direction, we can deem that the effective receive area A_e of each element in the array is

$$A_e = \eta_a A_p = \eta_a Db \tag{27}$$

So the gain of each element is

$$G(dB) = 4\pi \cdot \frac{A_e}{\lambda^2} \approx 30.2 \tag{28}$$

The evaluation above neglected the effect of some error sources, such as random surface errors, feed energy spillover. So the computed results would slightly deviate from the actual values.

4.4 Measurement Results

The whole antenna array system was manufactured and measured by us. The radiation patterns in two principal planes measured at the central frequency are given in Fig. 9. For brevity, here we only give the results of one element in the array. The radiation patterns for other elements are similar.

The sidelobe levels in H-plane are below the -20dB requirement, which are considered quite well, in particular, at the high frequency of Ka band. The synthetic power pattern incorporating array factor of ASR with element pattern in E-plane is given in Fig. 10 based on G-matrix method.

Table 3 shows the measured VSWR value of each element in the array at the central frequency.

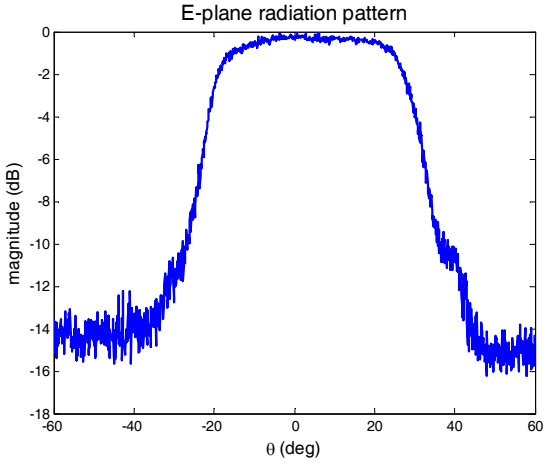

(a)

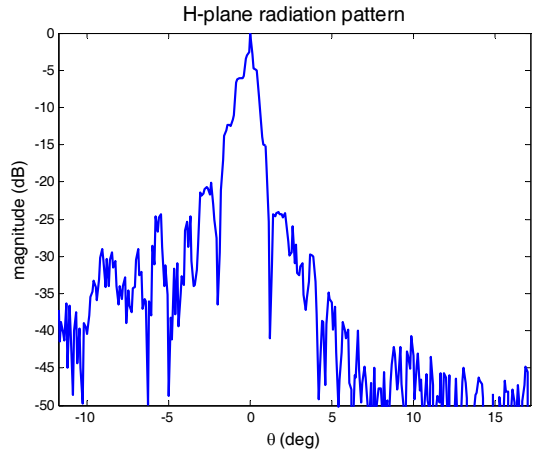

(b)

Fig. 9. Measured far field radiation pattern of antenna element; (a) E-plane, (b) H-plane

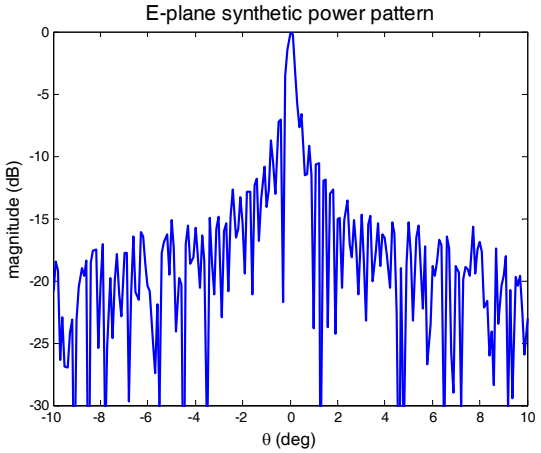

Fig. 10. E-plane synthetic power pattern by aperture synthesis

Element No.	VSWR	Element No.	VSWR
1	1.18	9	1.12
2	1.2	10	1.13
3	1.18	11	1.11
4	1.15	12	1.13
5	1.13	13	1.14
6	1.11	14	1.2
7	1.12	15	1.17
8	1.11	16	1.17

Table 3. Measured VSWR of each element in the array

All measured results indicate that the antenna array performs well with narrow main beamwidth, low peak sidelobe level and small VSWR, which are all desired for passive imaging radiometer.

5. Experiment Results with HUST-ASR

A series of experiments were conducted with HUST-ASR and brightness temperature images of natural scenes are shown in Fig. 11 and Fig. 12. In Fig. 11, natural scenes within a wide field of view are mapped. The outline of the chimney and the building nearby can be clearly distinguished. In Fig. 12, the outline and windows of the building and even the outline of the tree nearby can be seen in the image. Two air-conditioners on the wall of the building can also be seen in the image. All experimental results indicate that the HUST-ASR can generate good images of natural scenes with high spatial resolution provided by the antenna array.

Some "streaks" running along the vertical direction can be seen in the images due to the effect of slightly high sidelobes in H-plane pattern. Besides, our recent experimental work has shown that mutual effects of close antennas, as well as their individual matching, become important to fully understand the measurements. Thus, further research will be concentrated on error analysis and calibration of the antenna array in HUST-ASR.

(a)

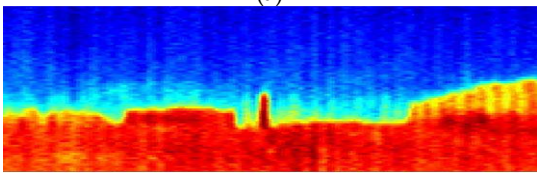

(b)

Fig. 11. Image of natural scenes within a wide FOV; (a) optic image; (b) brightness temperature image

(a)

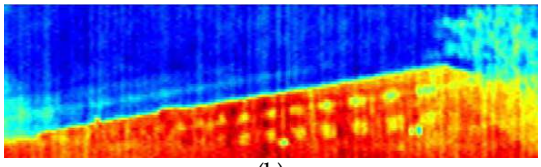

(b)

Fig. 12. (a) Optic image of a building; (b) brightness temperature image of a building

6. Conclusion

Antenna array design is an important issue for aperture synthesis radiometers (ASR). In this chapter, two subjects are mainly addressed: one is to optimize antenna array configurations, which determines the spatial sampling performance of ASR; the other is to design the antenna array in the practical ASR system as the performance of the antenna array has much influence on the radiometric imaging performance.

The topology optimization of the antenna array in ASR aims to find the minimum redundancy array (MRA), which can provide the most uniform and complete (u, v) coverage in the Fourier plane with the least number of antenna elements and therefore achieves the highest spatial resolution of the image. In this part, different optimization methods and different array configurations for both linear and planar arrays are summarized. And some original work by the authors, including the restricted search method by exploiting general structure of MRLAs and combinatorial methods for constructing thinned circular arrays, is also briefly presented.

As a second part of the chapter, a sparse antenna array with parabolic cylinder reflector at millimeter wave band for HUST-ASR prototype is presented. The overall specifications, architecture design, performance evaluation, and measurement results of the antenna array are all detailed. Measured results indicate that the antenna array performs well with narrow main beamwidth, low peak sidelobe level and small VSWR, which are all desired for passive imaging radiometers. Experimental results indicate that the HUST-ASR can generate good images of natural scenes with high spatial resolution provided by the antenna array. Further research will be concentrated on error analysis and calibration of the antenna array in HUST-ASR.

7. Acknowledgment

This work was supported in part by the National Science Foundation of China (NSF60705018) and in part by the National High Technology Research and Development Program of China (No. 2006AA09Z143). The authors would like to thank Prof. Wei Guo, Quanliang Huang, and Liangqi Gui for their enthusiastic encouragements, and thank my colleagues Ke Chen, Liang Lang, Fangmin He, Liangbin Chen, Zubiao Xiong, and Wei Ni for their helpful suggestion. The authors also thank Handong Wu, Yingying Wang in Xi'an Hengda Microwave Technology Corp. for their contributions to the work.

8. References

Balanis, C. A. (2005). *Antenna Theory-Analysis and Design,* 3rd ed., John Wiley & Sons Inc., New York

Baumert, L. D. (1971). *Cyclic Difference Sets,* Springer-Verlag, New York

Blanton, K. A.; McClellan, J. H. (1991). New search algorithm for minimum redundancy linear arrays. *Proceedings of IEEE ICASSP 1991,* Vol. 2, pp. 1361–1364

Bracewell, R. N. (1966). Optimum spacings for radio telescopes with unfilled apertures. *Natl. Acad. Sci. Natl. Res. Council. Publ.,* Vol. 1408, pp. 243–244

Butora, R.; Camps, A. (2003). Noise maps in aperture synthesis radiometric images due to cross-correlation of visibility noise. *Radio Sci.,* Vol.38, pp. 1067–1074

Camps, A. (1996). Application of interferometric radiometry fro earth observation. Ph. D. Eng. thesis, Univ. of Catalonian, Catalonian, Spain, Nov. 1996

Camps, A.; Bara, J.; Corbella, I.; Torres, F. A. (1997). The processing of hexagonally sampled signals with standard rectangular techniques: application to 2-D large aperture synthesis interferometric radiometers. *IEEE Trans. Geosci. Remote Sensing,* Vol. 35, No. 1, pp. 183-190

Camps, A.; Corbella, I.; Bara, J.; Torres, F. A. (1998). Radiometric sensitivity computation in aperture synthesis interferometric radiometry. *IEEE Trans. Geosci. Remote Sensing,* Vol. 36, No. 2, pp. 680-685

Camps, A.; Cardama, A.; Infantes, D. (2001). Synthesis of large low-redundancy linear arrays. *IEEE Trans. Antennas Propagat.,* Vol. 49, No. 12, pp. 1881–1883

Chen, C. Y.; Vaidyanathan, P. P. (2008). Minimum redundancy MIMO radars. *Proceedings of IEEE ISCAS 2008,* pp. 45–48

Chow, Y. L. (1970). Comparison of some correlation array configurations for radio astronomy. *IEEE Trans. Antennas Propagat.,* Vol. 18, pp. 567–569

Dong, J.; Li, Q. X.; Guo W.; Zhu Y. T. (2008a). A Sparse Antenna Array with Offset Parabolic Cylinder Reflector at Millimeter Wave Band, *Proceedings of IEEE ICMMT 2008*, pp. 1667-1670, Nanjin, China

Dong, J.; Li, Q. X.; He F. M.; Ni, W.; Zhu Y. T. (2008b). Co-array Properties of Minimum Redundancy Linear Arrays with Minimum Sidelobe Level, *Proceedings of IEEE ISAPE 2008*, pp. 74-77, Kunming, China

Dong, J.; Li, Q. X.; Guo W.; Zhu Y. T. (2009a). An Approach to Topology Design of Two Dimensional Sparse Arrays for Synthetic Aperture Interferometric Radiometer. *J. Microwave*, Vol.25, No. 2, pp. 83–86

Dong, J.; Li, Q. X.; Jin, R.; Huang, Q. L.; Gui, L. Q.; Zhu Y. T. (2009b). Difference Set Based Methods for Optimal Thinned Circular Arrays in Aperture Synthesis Radiometers. to be published in *J. Microwave*

Dong, J.; Li, Q. X.; Guo, W. (2009c). A Combinatorial Method for Antenna Array Design in Minimum Redundancy MIMO Radars. *IEEE Antennas Wireless Propagat. Lett.*, vol. 8, pp. 1150-1153, 2009.

Dong, J.; Li, Q. X.; Jin, R.; Zhu, Y. T.; Huang, Q. L.; Gui, L. Q. (2009d). A Method for Seeking Low-Redundancy Large Linear Arrays for Aperture Synthesis Microwave Radiometers. *IEEE Trans. Antennas Propagat.*, in press.

Dong, J.; Li, Q. X.; Gui, L. Q.; Guo, W. (2009e). The Placement of Antenna Elements in Aperture Synthesis Radiometers for Optimum Radiometric Sensitivity. *IEEE Trans. Antennas Propagat.*

Dorigo, M.; Stutzle, T. (2004). *Ant Colony Optimization,* MIT Press, Cambridge, MA

Dudgeon, D. E.; Mersereau R. M. (1984). *Multidimensional Digital Signal Processing,* Prentice-Hall Inc., New York

Ehrhardt, J. C. (1993). Hexagonal fast Fourier transform with rectangular output. *IEEE Trans. Signal Process.,* Vol.41, No. 3, pp. 1469–1472

Greene, C. R.; Wood, R. C. (1978). Sparse array performance. *J. Acoust. Soc. Amer.,* Vol.63, pp. 1866–1872

Goldberg, D. E. (1989). *Genetic Algorithms in Search, Optimization, and Machine Learning,* Addison-Wesley, Reading, MA

Hall, M. Jr. (1986). *Combinatorial Theory,* 2nd ed., John Wiley & Sons Inc., New York

Ishiguro, M. (1980). Minimum redundancy linear arrays for a large number of antennas. *Radio Sci.,* Vol.15, pp. 1163–1170

Jorgenson, M. B.; Fattouche, M.; Nichols, S. T. (1991). Applications of minimum redundancy arrays in adaptive beamforming. *Microwaves, Antennas and Propagation, IEE Proceedings H,* Vol. 138, pp. 441–447

Keto, E. (1997). The Shapes of Cross-correlation Interferometers. *The Astrophysical Journal,* Vol.475, pp. 843–852

Kopilovich, L. E. (1992). New approach to constructing two-dimensional aperture synthesis systems. *Radar and Signal Processing, IEE Proceedings F,* Vol.139, pp. 365–368

Kopilovich, L. E. (1995). Minimization of the number of elements in large radio interferometers. *R. Astron. Soc.,* Vol.274, pp. 544–546

Kopilovich, L. E.; Sodin, L. G. (1996). Aperture optimization of telescopes and interferometers: A combinatorial approach. *Astron. Astrophys. Suppl. Ser.,* Vol.116, pp. 177–185

Kopilovich, L. E. (2001). Configuration of a multielement interferometer covering hexagonal domains in the spatial-frequency plane. *Astron. & Astrophys.,* Vol.380, pp. 758–760

Lambrigtsen, B.; Wilson, W.; Tanner, A. B.; Gaier, T.; Ruf, C. S.; Piepmeier, J. (2004). GeoSTAR - a microwave sounder for geostationary satellites. *Proceedings of IEEE IGARSS 2004,* Vol. 2, pp. 777–780

Lee, Y.; Pillai, S. U. (1988). An algorithm for optimal placement of sensor elements. *Proceedings of IEEE ICASSP 1988,* Vol. 5, pp. 2674–2677

Lee, H. J.; Park, H.; Kim, S. H.; Kim, Y. H.; Kang, G. S. (2005). Evaluation of angular resolution in near field using two point targets for Ka-band interferometric synthetic aperture radiometer with sub-Y-type array configuration. *Proceedings of IEEE IGARSS 2005,* pp. 4921–4924

Leech, J. (1956). On the representation of 1,2,...,*n* by differences. *J. London Math. Soc.,* Vol.31, pp. 160–169

Le Vine, D. M. (1990). The sensitivity of synthetic aperture radiometers for remote sensing applications from space. *Radio Sci.,* Vol.25, pp. 441–453

Le Vine, D. M.; Griffs, A. J.; Swift, C. T.; Jackson, T. J. (1994). ESTAR: a synthetic aperture microwave radiometer for remote sensing applications. *Proceedings of The IEEE,* Vol. 82, No. 12, pp. 1787–1801

Le Vine, D. M.; Swift, C. T.; Haken, M. (2001). Development of the synthetic aperture microwave radiometer, ESTAR. *IEEE Trans. Geosci. Remote Sensing,* Vol. 39, No. 1, pp. 199–202

Li, Q. X.; Chen K.; Guo, W.; Lang L.; He F. M.; Chen L. B.; Xiong Z. B. (2008a). An Aperture Synthesis Radiometer at Millimeter Wave Band, *Proceedings of IEEE ICMMT 2008*, pp. 1699-1701, Nanjin, China

Li, Q. X.; Hu, F.; Guo, W.; Chen, K.; Lang, L.; Zhang, J.; Zhu, Y. T.; Zhang, Z. Y. (2008b). A General Platform for Millimeter Wave Synthetic Aperture Radiometers, *Proceedings of IEEE IGARSS 2008*, pp. 1156-1159, Boston, U.S.A.

Lin, C. L.; Nie, Z. P. (2002). *Antenna Engineering Handbook,* Electronic Industry House, Beijing

Linebarger, D. A. (1992). A fast method for computing the coarray of sparse linear arrays. *IEEE Trans. Antennas Propagat.,* Vol. 40, No. 9, pp. 1109–1112

Linebarger, D. A.; Sudborough, I. H.; Tollis, I. G. (1993). Difference bases and sparse sensor arrays. *IEEE Trans. Inform. Theory,* Vol. 39, No. 2, pp. 716–721

Mersereau, D. A. (1979). The processing of hexagonally sampled two-dimensional signals. *Proceedings of the IEEE,* Vol. 67, pp. 930–949

Miller, J. (1971). Difference bases, three problems in additive number theory. in *Computers in Number Theory,* London: Academic Press, pp. 229–322

Milligan, T. A. (2002). *Modern Antenna Design,* 2nd ed., John Wiley & Sons Inc., New Jersey

Mills, B. Y.; Little, A. G. (1953). A high resolution aerial system of a new type. *Aust. J. Phys.,* Vol.6, pp. 272

Martín-Neira, M.; Goutoule, J. M. (1997). A two-dimensional aperture-synthesis radiometer for soil moisture and ocean salinity observations. *ESA Bull.,* No. 92, pp. 95–104

Pearson, D.; Pillai, S. U.; Lee, Y. (1990). An algorithm for near-optimal placement of sensor elements. *IEEE Trans. Inform. Theory,* Vol. 36, No. 6, pp. 1280–1284

Pillai, S. U.; Bar-Ness, Y.; Haber, F. (1985). A new approach to array geometry for improved spatial spectrum estimation. *Proceedings of the IEEE,* Vol. 73, pp. 1522–1524

Rautiainen, K.; Kainulainen, J.; Auer, T.; Pihlflyckt, J.; Kettunen, J.; Hallikainen, M. T. (2008). Helsinki University of Technology L-Band Airborne Synthetic Aperture Radiometer. *IEEE Trans. Geosci. Remote Sensing,* Vol. 46, No. 3, pp. 717-726

Redéi, L.; Rényi, A. (1949). On the representation of 1,2,...,*n* by means of differences (in Russian). *Mat. Sbornik (Recueil Math.),* Vol.66(NS 24), pp. 385–389

Ruf, C. S.; Swift, C. T.; Tanner A. B.; Le Vine, D. M. (1988). Interferometric synthetic aperture radiometry for the remote sensing of the Earth. *IEEE Trans. Geosci. Remote Sensing,* Vol. 26, No. 5, pp. 597–611

Ruf, C. S. (1993). Numerical annealing of low-redundancy linear arrays. *IEEE Trans. Antennas Propagat.,* Vol. 41, No. 1, pp. 85–90

Sodin, L. G.; Kopilovich, L. E. (2001). Hexagonal configuration of cross-correlation interferometers. *Astron. & Astrophys.,* Vol.368, pp. 747–748

Sodin, L. G.; Kopilovich, L. E. (2002). Hexagonal arrays for radio interferometers. *Astron. & Astrophys.,* Vol.392, pp. 1149–1152

Tanner, A. B. (1990). Aperture synthesis for passive microwave remote sensing: The electronically steered thinned array radiometer. Ph. D. Eng. thesis, Univ. of Mass., Amherst, American, Feb. 1990

Tanner, A. B.; Swift, C. T. (1993). Calibration of a synthetic aperture radiometer. *IEEE Trans. Geosci. Remote Sensing,* Vol. 31, No. 1, pp. 257-267

Thompson, A. R.; Moran, J. M.; Swenson, G. W. Jr. (2001). *Interferometry and Synthesis in Radio Astronomy,* 2nd ed., John Wiley & Sons Inc., New York

Wichmann, B. (1963). A note on restricted difference bases. *J. London Math. Soc.,* Vol.38, pp. 465–466

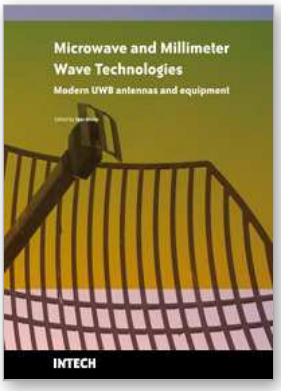

Microwave and Millimeter Wave Technologies Modern UWB antennas and equipment

Edited by Igor Mini

ISBN 978-953-7619-67-1
Hard cover, 488 pages
Publisher InTech
Published online 01, March, 2010
Published in print edition March, 2010

How to reference

In order to correctly reference this scholarly work, feel free to copy and paste the following:

Jian Dong and Qingxia Li (2010). Antenna Array Design in Aperture Synthesis Radiometers, Microwave and Millimeter Wave Technologies Modern UWB antennas and equipment, Igor Mini (Ed.), ISBN: 978-953-7619-67-1, InTech, Available from: http://www.intechopen.com/books/microwave-and-millimeter-wave-technologies-modern-uwb-antennas-and-equipment/antenna-array-design-in-aperture-synthesis-radiometers

INTECH
open science | open minds

InTech Europe
University Campus STeP Ri
Slavka Krautzeka 83/A
51000 Rijeka, Croatia
Phone: +385 (51) 770 447
Fax: +385 (51) 686 166
www.intechopen.com

InTech China
Unit 405, Office Block, Hotel Equatorial Shanghai
No.65, Yan An Road (West), Shanghai, 200040, China
中国上海市延安西路65号上海国际贵都大饭店办公楼405单元
Phone: +86-21-62489820
Fax: +86-21-62489821